 Bull. Chem. Soc. Jpn. Vol. 79, No. 10, 1607–1613 (2006)

Systematic Studies on Chain Lengths, Halide Species, and Well Thicknesses for Lead Halide Layered Perovskite Thin Films

Yuko Takeoka,*[1,2] Keisuke Asai,[3] Masahiro Rikukawa,[1] and Kohei Sanui[1]

[1]Department of Chemistry, Sophia University, 7-1 Kioi-cho, Chiyoda-ku, Tokyo 102-8554

[2]Department of Applied Chemistry, Tohoku University, Aoba, Aramaki, Aoba-ku, Sendai 980-8579

[3]PRESTO, Japan Science and Technology Agency (JST), 4-1-8 Hon-cho, Kawaguchi 332-0012

Received March 10, 2006; E-mail: y-tabuch@sophia.ac.jp

Two-dimensional layered perovskite compounds, $(C_nH_{2n+1}NH_3)_2(CH_3NH_3)_{m-1}Pb_mX_{3m+1}$ ($n = 2$, 3, 4, 6, and 10; X = Cl, Br, and I; $m = 1$, 2, and 3) were systematically prepared. The influences of the barrier-size, halide species, and well thickness of the perovskite thin films on the quantum confinement structures were investigated. The layered perovskite films showed a strong and clear absorption peak due to excitons confined in inorganic quantum-wells. The exciton peak shifted to lower energy as the halide species was changed from Cl to Br and I. Furthermore, fine multilayer perovskite compound films were prepared by varying the spin-coating conditions.

Low-dimensional systems can be readily constructed by a simple method involving organic–inorganic hybrid materials without using the large-scale pieces of apparatus needed by conventional techniques.[1,2] Organic materials with specific functionality are combined on a molecular scale with an inorganic matrix with other target properties, creating an organic–inorganic hybrid with either a combination of useful properties or new phenomena arising from the interaction between organic and inorganic components. Organic–inorganic perovskite-type compounds are one of the versatile hybrid materials that are currently studied by many groups due to their potential for unique electrical, magnetic, and optical properties.[3,4]

The most commonly studied system with the general formula $(C_nH_{2n+1}NH_3)_2PbX_4$ (X: halide) naturally forms a layered structure consisting of two-dimensional sheets of $[PbX_6]^{4-}$ octahedra and organic ammonium ($C_nH_{2n+1}NH_3^+$) layers.[5,6] The layered structure is self-organized via hydrogen bonds between the inorganic sheet halogens and the organic ammonium groups and also via van der Waals interactions between adjacent organic tails. Since the bandgap of the organic layers is much larger than that of the inorganic layer based on $[PbX_6]^{4-}$ octahedra (by at least 3 eV), the organic layers in this system act as insulating barrier layers, and the inorganic layers behave as semiconductor layers. The interfaces between the inorganic and organic layers are intrinsically flat, and it is thought that excitons are confined to behave as an ideal two-dimensional system. In fact, the existence of very stable excitons with extremely large exciton binding energy (320 meV) and oscillator strength (≈0.7) was reported for $(C_6H_{13}NH_3)_2PbI_4$.[7] The stable excitons provide excellent optical properties, such as strong photoluminescence and high optical nonlinearity, which makes the family of organic–inorganic layered perovskites a promising and growing research field.[8–11]

Another unique feature of these materials is the tunability of their nano structures.[12–14] For example, although two-dimensional structures are found in $(C_nH_{2n+1}NH_3)_2PbX_4$, a three-dimensional (3-D) structure is constructed by using smaller alkylamines such as NH_4^+ and $CH_3NH_3^+$.[15,16] With this approach, it is possible to create new materials with different dimensional structures that vary from zero to three, all using the same simple combination of organic amines and metal halides.[17] In addition to these one- to three-dimensional structures, the existence of intermediate dimensionality structures with variable well thicknesses, $(C_nH_{2n+1}NH_3)_2(CH_3NH_3)_{m-1}M_mX_{3m+1}$, has been reported.[18] In these structures, methylammonium ($CH_3NH_3^+$) fits into the center of eight MX_6 corner-shared octahedra, while a long-chain alkylammonium RNH_3^+ fits only into the periphery of a set of four MX_6 octahedra. To maintain charge neutrality, methylammonium ions incorporate into the inorganic framework and serve as counter-ions to make the two layers cohere. The multilayer $CH_3NH_3MX_3$ perovskite sheets are sandwiched between the $[C_nH_{2n+1}NH_3]^+$ layers.[19,20] Mitzi et al. also discovered that there was a metal–semiconductor transition in $(C_nH_{2n+1}NH_3)_2(CH_3NH_3)_{m-1}Sn_mX_{3m+1}$, dependent on the thickness of the inorganic perovskite sheets.[21,22] These intermediate dimensionality structures form natural multi-quantum-well structures with variable well thickness (controlled by m) and even well depth (controlled by the halogen), providing an ideal model for tailoring the optical and electrical properties.

To explore the effects of well-size, barrier-size, and well-thickness (multilayer) on the structural, thermal, and optical properties using this series of layered perovskite compounds, we have performed extended systematical studies which are shown in Scheme 1. Although several studies involving this series of compounds have been reported, most of them focused on one scientific matter, and it was difficult to investigate the relationships between the properties and the structures throughout the entire compound and to show the correlations among the three different phases. Extremely pure compounds, $(C_nH_{2n+1}NH_3)_2(CH_3NH_3)_2Pb_3X_{10}$ (X = Cl, Br, and I), with multi-layer inorganic sheets ($m \geq 3$) have not yet been

Published on the web October 10, 2006; doi:10.1246/bcsj.79.1607

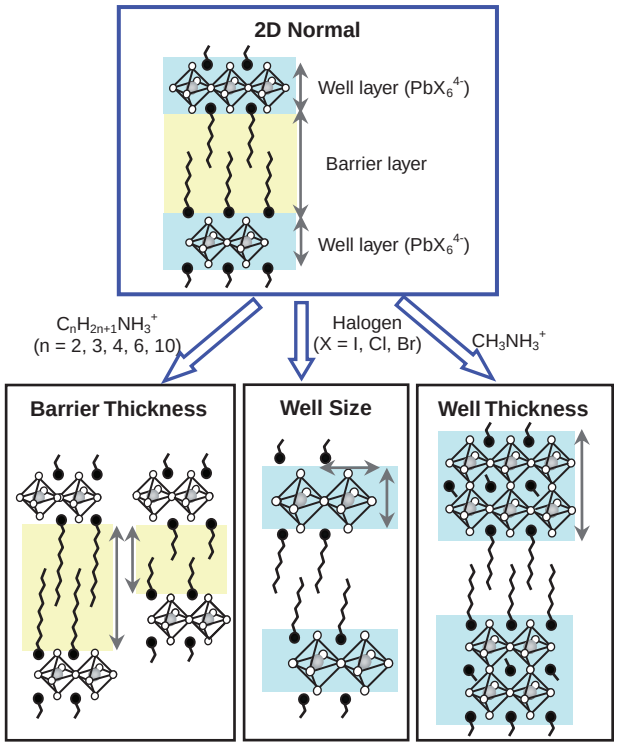

Scheme 1. Schematic view of this study with layered perovskites which explores the effects of barrier-thickness, well-size, and well-thickness on their structural, thermal, and optical properties.

obtained due to the difficulty in stoichiometrically controlling the inorganic and organic components. We, herein, attempted the fabrication of $(C_nH_{2n+1}NH_3)_2(CH_3NH_3)_{m-1}Pb_mX_{3m+1}$ (X = Cl, Br, and I), which has mono ($m = 1$), bi ($m = 2$), and tri ($m = 3$) layer structures of inorganic two-dimensional sheets. Furthermore, a systematic study was undertaken to determine whether desired crystalline structures could be prepared and to establish the optimum conditions for the preparation of multi-layered compounds.

Experimental

Materials. *n*-Alkylamines and hydrohalogenic acids (HCl 35 wt %, HBr 48 wt %, and HI 57 wt %) were obtained from Wako Pure Chemical Industries, Ltd. Lead halides (PbX_2, X = I, Br, and Cl, purity ≥ 99.99%) were purchased from Kojundo Chemical Laboratory Co., Ltd. and were used as received. A series of alkylammonium salts were prepared by reacting *n*-alkylamine with a stoichiometric amount of hydrohalogenic acid aqueous solution for 3 h at room temperature, and the crude product was recrystallized from methanol. The layered perovskite-type compounds were prepared as follows.

Monolayer Compounds, $(C_nH_{2n+1}NH_3)_2PbX_4$. $(C_nH_{2n+1}NH_3)_2PbI_4$: The PbI-based monolayer ($m = 1$) perovskites, $(C_nH_{2n+1}NH_3)_2PbI_4$ (C_nPbI_4, $n = 2$, 3, 4, 6, and 10), were prepared by treating the corresponding $C_nH_{2n+1}NH_3I$ with a stoichiometric amount of PbI_2. $C_nH_{2n+1}NH_3I$ (5.0 mmol) was dissolved in acetone (10 mL) at room temperature. PbI_2 (1.15 g, 2.5 mmol) was then added to this solution under nitrogen. The reaction solutions were stirred for 1 h after the PbI_2 was completely dissolved. The solution was poured into nitromethane, and the microcrystalline powder that found was collected by filtration. C_nPbI_4 ($n = 2$ and 3) cannot be collected as powder samples. C_nPbBr_4 and C_nPbCl_4 were prepared in a similar manner to C_nPbI_4, but the solvents were different. *N*,*N*-Dimethylformamide (DMF) was used as the reaction solvent for C_nPbX_4 (X = Br and Cl), and powder samples were obtained by pouring the reaction solutions into acetone. The yield of C_nPbX_4 was ca. 70%. Anal. Calcd for $C_{12}H_{32}N_2PbBr_4$: C, 19.71; H, 4.41; N, 3.83%. Found: C, 19.80; H, 4.47; N, 3.80%.

Bilayer Compounds, $(C_6H_{13}NH_3)_2(CH_3NH_3)Pb_2X_7$. The bilayer ($m = 2$) perovskite, $(C_6H_{13}NH_3)_2(CH_3NH_3)Pb_2I_7$ ($C_6Pb_2I_7$), was prepared by reacting stoichiometric amounts of $C_6H_{13}NH_3I$ and CH_3NH_3I with PbI_2. CH_3NH_3I (2.5 mmol) and $C_6H_{13}NH_3I$ (5.0 mmol) were dissolved in DMF (20 mL) at 35 °C in advance. After the two amines were dissolved completely in DMF, PbI_2 (5.0 mmol) was added to the solutions and reacted for 1 h under nitrogen. Then, the reaction solutions were poured into nitromethane (X = I) to precipitate the product. Centrifugal separation was used because the bilayer compounds were too fine to separate by filtration. The analogous halide compounds, $C_6Pb_2X_7$ (X = Br and Cl) were synthesized similarly, except that the reaction solutions were poured into acetone to precipitate the product. The yield of $C_6Pb_2X_7$ was approximately 60%. Anal. Calcd for $C_9H_{27}N_3Pb_2Br_7$: C, 9.37; H, 2.62; N, 3.64%. Found: C, 9.36; H, 2.59; N, 3.67%.

Trilayer Compounds, $(C_6H_{13}NH_3)_2(CH_3NH_3)_2Pb_3X_{10}$. Pure trilayer compound, $(C_6H_{13}NH_3)_2(CH_3NH_3)_2Pb_3I_{10}$ ($C_6Pb_3I_{10}$), was obtained only when the reaction was carried out at 35 °C with a feed ratio of $C_6H_{13}NH_3I$:CH_3NH_3I:PbI_2 = 2:3:3. CH_3NH_3I (7.5 mmol) and $C_6H_{13}NH_3I$ (5.0 mmol) were at first dissolved in DMF (30 mL) at 35 °C. After the two amines were completely dissolved, PbI_2 (7.5 mmol) was added to the mixed solutions. The reaction solutions were poured into nitromethane. $C_6Pb_3I_{10}$ was obtained as a powder by centrifugation in a procedure similar to that described above. The compounds $C_6Pb_3X_{10}$ (X = Br and Cl) were synthesized similarly except that acetone was used instead of nitromethane. The yield of $C_6Pb_3X_{10}$ was approximately 60%.

Three-Dimensional Compounds $CH_3NH_3PbX_3$. The three-dimensional perovskite ($m = \infty$) $CH_3NH_3PbI_3$ was synthesized by reacting a stoichiometric amount of PbI_2 with CH_3NH_3I. A mixed solution of CH_3NH_3I (5.0 mmol) and PbI_2 (5.0 mmol) in DMF (10 mL) was prepared at room temperature. When the reaction solution was poured into nitromethane, microcrystalline $CH_3NH_3PbI_3$ precipitated. The compounds $CH_3NH_3PbX_3$ (X = Br and Cl) were synthesized similarly except for the use of acetone for the reprecipitation. The yields of $CH_3NH_3PbX_3$ were approximately 90%. Anal. Calcd for CH_6NPbBr_3: C, 2.51; H, 1.25; N, 2.92%. Found: C, 2.41; H, 1.34; N, 2.81%.

Film Preparation. DMF solutions of crystalline powder were prepared and were filtered with a 0.5 μm filter prior to use. Films were fabricated on hydrophilic substrates by spin-coating at approximately 6000 r.p.m. using a MIKASA 1H-D7. The substrates were heated at ca. 60 °C during the spin-coating process to obtain high quality films due to the high boiling point of DMF. $C_6Pb_3X_{10}$ spin-coated films could not be obtained from solutions that were prepared from the powder sample. The $C_6Pb_3X_{10}$ films were obtained directly using the reaction solution.

Structural Analysis. Optical absorption spectra of the spin-coated films were obtained on a U-3300 spectrophotometer (Hitachi) at room temperature. Fluorescence spectra were recorded on an F-3000 spectrophotometer (Hitachi) at different excita-

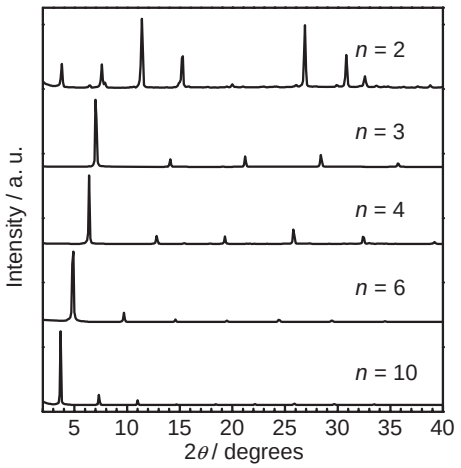

Fig. 1. X-ray diffraction patterns of $(C_nH_{2n+1}NH_3)_2PbBr_4$ ($n = 2$, 3, 4, 6, and 10) spin-coated films at room temperature.

tion wavelengths (300 nm for X = Br and Cl, 310 nm for X = I). X-ray diffraction measurements were performed over a 2θ range of 1.5 to 40° using a Rigaku RINT2000 diffractometer with a Ni-filtered copper Kα target ($\lambda = 1.5418$ Å) at 40 kV and 25–40 mA. Simultaneous thermogravimetric and differential thermal analyses (TG-DTA) was conducted for the freshly prepared powders on TG-DTA200 (Seiko) under a nitrogen flow of 200 mL min^{-1}. Differential scanning calorimetry (DSC) thermograms were also collected on a DSC200 (Seiko) under a nitrogen flow of 40 mL min^{-1}. The topology and microstructure of $C_nPb_mX_{3m+1}$ spin-coated films were examined by atomic force microscopy (AFM). AFM measurements were performed on a Nanoscope IIIa (Digital Instruments) operating in the tapping mode.

Results and Discussion

Synthesis and Structural Analysis of Monolayer Perovskite Compounds $(C_nH_{2n+1}NH_3)_2PbX_4$. Layered perovskite-type compounds, $(C_nH_{2n+1}NH_3)_2PbX_4$ (C_nPbX_4), were systematically synthesized with various $C_nH_{2n+1}NH_3X$ and PbX_2 materials. The powders that were obtained were white (X = Cl and Br) and orange (X = I), and polycrystalline thin films of the compounds were easily fabricated by spin-coating. At first, to examine the effects of alkyl chain length on the layered structures, we prepared monolayer C_nPbX_4 films with various alkylamines ($n = 2$, 3, 4, 6, and 10) in the organic layers. Figure 1 shows the X-ray diffraction patterns obtained from the C_nPbBr_4 spin-coated films that have $PbBr_4$ inorganic sheets. A series of (00l) diffraction peaks corresponding to the interlayer spacing was clearly observed, indicating the formation of a two-dimensional layered structure for each sample. The PbCl and PbI-based systems also exhibited similar X-ray diffraction patterns, suggesting primarily *c*-axis orientation. Table 1 shows the interlayer spacings for C_nPbX_4 calculated from the X-ray diffraction patterns using the Bragg equation. Since the layer spacings increase linearly with increasing the alkyl chain length in all these monolayer perovskite samples, the interlayer spacing l can be expressed as: l (Å) = $a + bn$, where n is the number of carbon atoms in the alkylamine; $a = 7.32$, 8.06, and 9.27; $b = 1.79$, 1.59, and 1.21 for X = Cl, Br, and I, respectively. The chain length of a normal hydrocarbon chain is considered to increase by 2.5 Å per carbon atom, assuming that the alkyl chain is oriented with the lowest energy. The increment of the layer spacing value b is much smaller than 2.5 Å each case. As described above, the order of the b values is $C_nPbCl_4 > C_nPbBr_4 > C_nPbI_4$ within the n range examined in this study. Also, note that the a value, which corresponds to the layer spacing of the three-dimensional compounds, is larger than that of the corresponding cubic perovskite compounds, and its order is $C_nPbCl_4 < C_nPbBr_4 < C_nPbI_4$. These results suggest that the larger halogen atom in the $[PbX_6]^{4-}$ layer provides more space parallel to the organic layer surface, which leads to the tilting and/or interdigitating of the alkyl chains.

Table 1. Interlayer Spacing Obtained from X-ray Diffraction and Absorption Band of $(C_nH_{2n+1}NH_3)_2PbX_4$ (X = Cl, Br, and I)

	d-Spacing/Å			Exciton peaks/nm		
n	Cl	Br	I	Cl	Br	I
2	11.3	11.6	11.9	329	392, 420	—
3	12.6	12.6	13.0	331	402	505
4	14.0	14.0	13.8	330	403	509
6	18.4	18.0	16.1	330	395	512
10	25.2	23.9	21.5	329	388	509

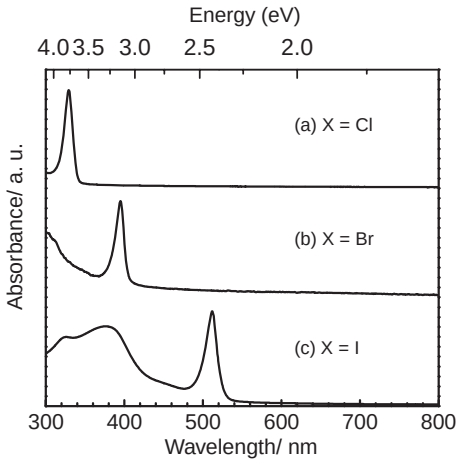

Fig. 2. Optical absorption spectra of $(C_6H_{13}NH_3)_2PbX_4$ (X = Cl, Br, and I) spin-coated films at room temperature.

The optical absorption spectra of the monolayer ($m = 1$) compounds, C_6PbX_4, were measured at room temperature to examine the effect of changing halogen atom on the optical properties of these perovskite compounds. The monolayer films have a strong and sharp absorption at 330 (X = Cl), 395 (X = Br), and 512 nm (X = I), even at room temperature, as shown in Fig. 2. Because neither PbX_2 nor $C_6H_{13}NH_3X$ have absorption peaks in the vicinity of the peaks exhibited by C_6PbX_4, the characteristic peaks in the monolayer films are attributed to an exciton in the $[PbX_6]^{4-}$ inorganic layer, which is sandwiched between organic barrier layers. The fact that the excitons can be observed even at room temperature is demonstrative of the high stability of the exciton states in these monolayer films. The exciton peak red-shifted as the halogen atom was changed from Cl to Br to I. This red shift is attributed to the change of the energy-gap for the corre-

sponding inorganic perovskites, indicating that the optical properties can be tailored by changing the halogen species.

The effect of the distance between the inorganic layers of two-dimensional materials on the electronic structures was investigated by comparing the exciton peaks in the optical absorption spectra. The exciton absorption for C_nPbX_4 films varied according to the changes in the halogen species, whereas no significant change was observed in the exciton absorption with any of the alkylamines examined. As summarized in Table 1, the C_nPbX_4 films with $n = 3$, 4, 6, and 10 had a single clear exciton peak at around 510 nm for X = I, at 395 nm for X = Br, and at 330 nm for X = Cl. Even if the distance between the adjacent lead halide layers decreases to $n = 3$, the qualitative features of the absorption spectra are essentially the same. This demonstrates that the distance between the inorganic layers with $C_3H_7NH_2$ as the organic components is enough to confine the exciton within the inorganic layers, in other words, the interaction between the inorganic layers is too weak to overlap with each other for C_nPbX_4 with three or more alkyl chains. In contrast, the C_2PbX_4 film with $C_2H_5NH_2$ exhibits a different phenomenon, i.e., the exciton absorption is dependent on the halogen type. Although the C_2PbCl_4 film had a single sharp peak attributable similar to a two-dimensional structure, the C_2PbBr_4 film had two absorption peaks at 390 and 402 nm that associated with the X-ray diffraction results, and the C_2PbI_4 has a very broad peak at around 520 nm (Fig. 3). This phenomenon can be explained by the following. The distances between the inorganic quantum-wells in C_2PbBr_4 and C_2PbI_4 films are not large enough to prevent percolation of the wave function, which is due to the interaction with the neighboring inorganic layers; therefore, these films did not show a clear exciton absorption. This is caused by the difference in the bandgap energy and electron affinity between the halogens. Electron affinity (E_a) and ionic potential (I_p) decrease as the halogen atom changes from Cl to Br to I. Accordingly, the electronegativity χ ($=(I_p + E_a)/2$) decreases, which means that the covalent bond character becomes stronger than the ionic character. Based on this reason, the ability of fabricating a two-dimensional confinement structure for a series of C_nPbX_4 follows Cl > Br > I. For the C_2PbCl_4 film with a large bandgap energy, the quantum-well made up of $[PbCl_6]^{4-}$ is deep enough to prevent the percolation of the wave function and to maintain the two-dimensional exciton features.

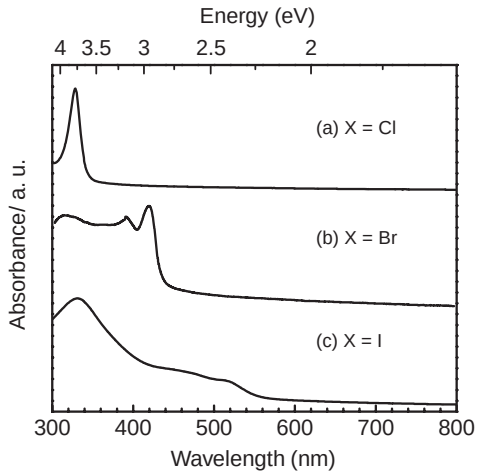

Fig. 3. Optical absorption spectra of $(C_2H_5NH_3)_2PbX_4$ (X = Cl, Br, and I) spin-coated films at room temperature.

Thermal Analysis of Monolayer Perovskite Compounds. The thermal decomposition behavior of the monolayer perovskite compounds was investigated by simultaneous thermogravimetric analysis (TGA) and differential thermal analysis (DTA). The decomposition temperatures of the standard layered compounds, C_4PbX_4, were 232, 276, and 270 °C for X = Cl, Br, and I, respectively. The X = I and Br compounds with butylammonium cations tend to be more thermally stable than that of X = Cl. We observed weight loss (20%) upon heating the C_4PbBr_4 to 310 °C and a somewhat larger weight loss above 310 °C. If the observed weight loss is due to the decomposition of the organic components ($C_4H_9NH_3^+$), the estimated weight loss of C_4PbBr_4 is 22%. Several thermal studies on the layered perovskites with various alkylamines were undertaken in which it was demonstrated that all of these layered perovskite compounds are stable to 200 °C. Also, note that the thermal stability depends on the orientation of the alkyl chains in the organic sheet. The Br and I compounds with the larger tilt angles (smaller layer spacing) have the higher thermal stability. The phase transition behavior of the layered perovskite compounds based on PbX_2 was also investigated. Table 2 summarizes the thermal transition peaks observed in the DSC thermograms of monolayer perovskites, C_nPbX_4. The transition temperatures are dependent on the chain length of the organic components and halogen atoms. C_4PbX_4 (X = Cl, Br, and I) exhibited no structural phase transitions below room temperature on the cooling scans. This is an important feature for practical applications in optical devices because the exciton peak does not skip at low temperatures. Owing to the differences in the PbX_2 matrices, the phase-transition behavior is not constant for a given chain length. Some trends for the transition temperatures can be found in these results. The C_nPbX_4 with relatively shorter or longer alkyl chains exhibit plural and lower transition peaks. In other words, there is a critical point in the transition temperatures

Table 2. Thermal Transitions of $(C_nH_{2n+1}NH_3)_2PbX_4$ from DSC Thermograms[a)]

C_nPbX_4	n	Transition point/°C	
		Heating Scan	Cooling
(a) X = Cl	3	5.8, 67, 96	61, 91
	4	53	47
	6	−57, 4.5, 31	−20, 27
	10	14, 55	8.4, 49
(b) X = Br	3	−102, −5.3	−110, 3.6
	4	110	107
	6	−87, −74, −48, 24	−54, 22
	10	−7.0, 54	−14, 45
(c) X = I	3	—	—
	4	1.1	−23
	6	10, 83, 102	76, 98
	10	14, 55	8.4, 49

a) $(C_3H_7NH_3)_2PbI_4$ cannot be collected as a powder.

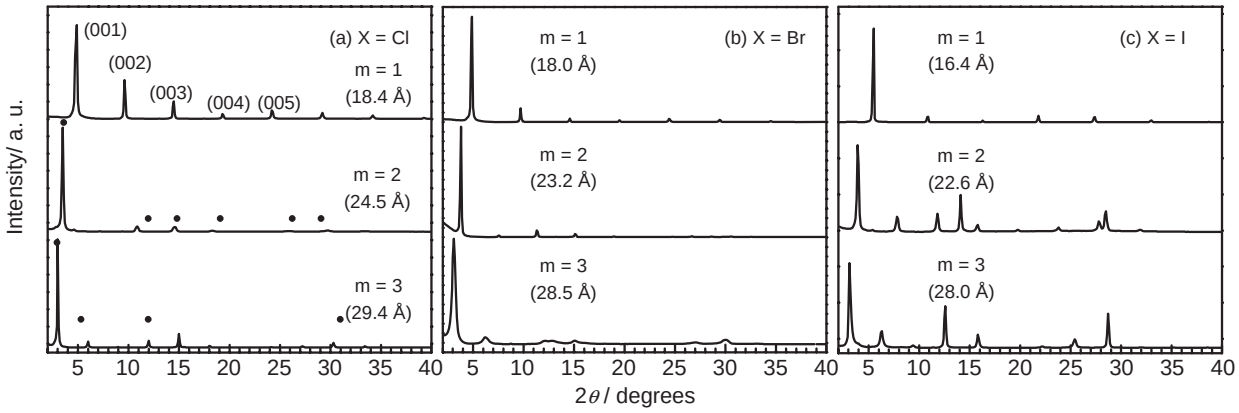

Fig. 4. X-ray diffraction patterns of $(C_6H_{13}NH_3)_2(CH_3NH_3)_{m-1}Pb_mX_{3m+1}$ ($m = 1$, 2, and 3) spin-coated films with (a) X = Cl, (b) Br, and (c) I at room temperature.

for the series of perovskites with different alkyl chains. As noted above, the C_4PbX_4 had a single and relatively high transition point on the both scans. This phenomenon can be explained by assuming that the spatial organization of the organic layers is determined by the size of halogen atoms and the length of alkyl chains. When a larger halogen atom is used for the fabrication of the perovskite, the space for the organic layers in the organic–inorganic frameworks necessarily enlarges. Shorter alkyl chains are loosely packed; consequently, plural and lower transition temperatures are observed as described above. In contrast, longer alkyl chains readily tilt and/or interdigitate, and a part of them are also loosely packed. Therefore, they have plural and lower transition points. Thus, the use of alkyl ammoniums with the intermediate chain lengths and adequate halogen atoms has somewhat tighter packing than for the other chain lengths, resulting in thermally stable perovskite compounds with single and higher transition points.

Synthesis and Structural Analysis of Multilayered Perovskite Compounds. Multilayered perovskite compounds with different inorganic layer thicknesses, $(C_nH_{2n+1}NH_3)_2(CH_3NH_3)_{m-1}Pb_mX_{3m+1}$ (Abbreviated to $C_nPb_mX_{3m+1}$, $m =$ 1–3), were fabricated using two alkylammonium materials having different alkyl chain lengths, ($C_nH_{2n+1}NH_2$ and CH_3NH_2), with a controlled ratio between them. Monolayer ($m = 1$) and bilayer ($m = 2$) perovskite compounds were prepared by the stoichiometric reaction ($C_nH_{2n+1}NH_2$:CH_3NH_2 = 2:0 and 2:1), whereas pure trilayer ($m = 3$) compounds can not be obtained by the stoichiometric reaction. The optimum experimental conditions for preparing the trilayer films were investigated by reacting $C_nH_{2n+1}NH_3X$, CH_3NH_3X, and PbX_2 at various molar ratios and directly spin-coating the reacting solutions. Note that the $C_nH_{2n+1}NH_3X/PbX_2$ molar ratio was fixed at 1.5 and the $C_nH_{2n+1}NH_3X$:CH_3NH_3X:PbX_2 molar ratios were changed within 2:2 to 3.5:3. Small variations in the molar ratio had significant effects on the structure of multilayer compounds. It was found from the optical analysis and structural results that the spin-coated films fabricated from a mixed solution of $C_nH_{2n+1}NH_3X$:CH_3NH_3X:PbX_2 in a molar ratio at 2:3:3 had the purest trilayer structure. Moreover, similar results were obtained for all other halogen analogues (X = Cl, Br, and I). Each solution of $C_nH_{2n+1}NH_3X$ and CH_3NH_3X was maintained at a temperature of 35 °C before adding the PbX_2 powder to obtain high quality trilayer, $C_nPb_3X_{10}$, films.

Table 3. Interlayer Spacing Obtained from X-ray Diffraction and Absorption Band of $(C_6H_{13}NH_3)_2(CH_3NH_3)_{m-1}Pb_mX_{3m+1}$ (X = Cl, Br, and I)

	d-Spacing/Å			Exciton peaks/nm		
Sample	Cl	Br	I	Cl	Br	I
Monolayer ($m = 1$)	18.4	18.0	16.4	330	395	512
Bilayer ($m = 2$)	25.2	23.2	22.6	349	431	569
Trilayer ($m = 3$)	29.4	28.5	28.0	356	450	604
Cubic ($m = \infty$)	5.68	5.80	6.28	397	528	740

Otherwise, other multilayer compounds $C_nPb_mX_{3m+1}$ ($m = 1$, 2, and ≥ 4) are easily produced as contaminants. Figure 4 shows the X-ray diffraction patterns of $C_6Pb_mX_{3m+1}$ spin-coated films with $m = 1$, 2, and 3 fabricated using optimum conditions. A series of diffraction patterns of the (00l) plane is clearly observed in all films. This observation strongly supports the facts that these films are highly oriented with the *c*-axis perpendicular to the substrate and that the perovskite films are well-crystallized. In the cases of $m = 2$ and 3, no diffraction peaks corresponding to the lower order or the higher order structure were detected by the X-ray diffraction measurements. The interlayer *d*-spacing values calculated from the X-ray diffraction results were 18.0, 23.2, and 28.5 Å for $C_6Pb_mBr_{3m+1}$ ($m = 1$, 2, and 3), respectively. The increments in the layer spacings observed between each system were 5.2 Å for the mono-bilayer and 5.3 Å for the bi-trilayer. The thickness of one $[PbBr_6]^{4-}$ octahedra layer was calculated to be 5.9 Å based on the lattice constant of the cubic perovskite $CH_3NH_3PbBr_3$.[23] Therefore, these X-ray diffraction results clearly demonstrate that the obtained spin-coated films consist of multilayered structure with mono, bi, or trilayers of inorganic sheets. Table 3 lists the *d*-spacing values of these multilayer films as calculated from the X-ray diffraction measurements. Although a similar increment in the *d*-spacing was observed in the X-ray diffraction patterns, the Cl and I systems showed longer and shorter increments than the thickness of $[PbX_6]^{4-}$ calculated from the cubic perovskite compounds.

Morphology of Two-Dimensional Thin Films with Multilayer Quantum-Wells. Figure 5 shows the AFM topology images of $C_6Pb_mBr_{3m+1}$ ($m = 1$, 2, 3, and ∞). In each spin-coated film, polycrystalline grains covered the substrate, while grain morphology was quite different and was dependent on

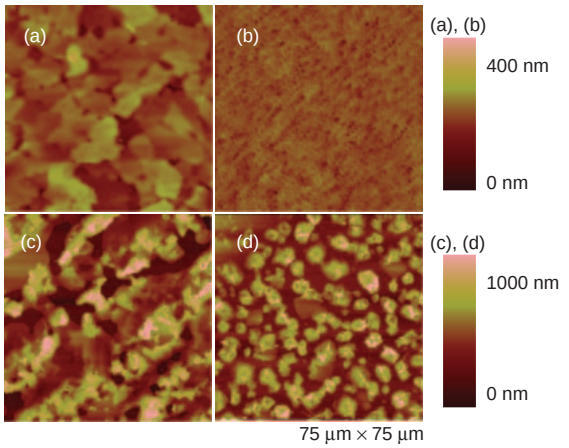

Fig. 5. Tapping mode AFM topology images of $(C_6H_{13}NH_3)_2(CH_3NH_3)_{m-1}Pb_mBr_{3m+1}$ spin-coated films with (a) $m = 1$, (b) $m = 2$, (c) $m = 3$, and (d) $m = \infty$.

the compositions. The monolayer compounds form plate-like crystals with an average long side length of about 10 μm (Fig. 5a), highlighting the fact that a layered structure can be formed with the perovskite sheets approximately parallel to the substrate. This is consistent with the results that the X-ray diffraction patterns in which only (00l) reflections were observed in Fig. 4. In the $m = \infty$ compounds (Fig. 5d), square-like crystals were observed with an average dimension of 3–5 μm. The morphology of the layered perovskites with multi-layer quantum wells was affected dramatically by the inorganic sheet width m in the layered structure. For the bilayer compounds, the surface was covered by fine grains like a herringbone, which proves the fact that the bilayer compounds are too fine to collect by filtration, as described in Experimental Section. By contrast, plate-like grains were also observed for the trilayer films. The morphology of trilayer films appeared to be smaller and to distribute more randomly compared to the monolayer films. Since excess CH_3NH_3Br may exist in the trilayer films, it would prevent the crystallization and growth of the trilayer crystals. This result was consistent with the fact that the half-width of the X-ray diffraction peak for the trilayer film is slightly wider than that of the mono or bilayer films, as shown in Fig. 4.

Optical Properties of Two-Dimensional Thin Films with Multilayer Quantum-Wells. The optical absorption spectra of the $C_6Pb_mX_{3m+1}$ ($m = 1$, 2, 3, and ∞; X = Cl, Br, and I) spin-coated films were measured at room temperature. The exciton absorption peaks of these films are listed in Table 3. Each spin-coated film has a strong absorption peak corresponding to the lowest exciton states; the form of the peaks is due to the inorganic semiconductor wells confined by electronic potential and dielectric confinement. In all of the halogen systems, the absorption peaks of $C_6Pb_mX_{3m+1}$ red-shifted as the inorganic layer thickness, m, increased. There are two possible reasons for the red shift. The first reason is a decrease in the quantum confinement effect due to the expansion of the exciton Bohr radius, resulting in a decrease in exciton binding energy. The second reason is a decrease in the bandgap.[24] As the inorganic sheet thickness increases, the conduction and valence bands become wider because the transfer energy between $[PbX_6]^{4-}$ octahedra becomes larger. The red shifts of exciton peaks from monolayer to bilayer compounds can be explained by this model. However, it is impossible to apply this model to the trilayer compounds because only the interaction between adjacent $[PbX_6]^{4-}$ octahedra is taken into consideration in this model. The $[PbX_6]^{4-}$ octahedra in the trilayer compounds have been divided into two types: Octahedra in the exterior layers is contact with five $[PbX_6]^{4-}$ units and the ones in the center layers is contact with six units. The transfer energy of the former type is similar to the bilayer compounds, while the latter type is similar to the 3D compounds. If we take this model into consideration, the trilayer compounds are thought to have two absorption bands. The trilayer compounds actually have a single absorption peak, which does not originate from the bilayer or cubic compounds. Therefore, an alternative picture based on delocalized excitations is needed in the compounds with $m \geq 3$. In other words, a unified picture combining the localized excitations for $m \leq 2$ and the delocalized ones for $m \geq 3$ should be constructed. A shift in the exciton peak was observed as the halogen was changed from Cl to Br to I, which was identical to those described in Fig. 2. The excitonic bands in the chloride compounds arise at smaller energies than those of the corresponding bromide and iodide compounds. This is due to the decrease in the bandgap as the halogen changes from Cl to Br and I. While the exciton peaks of the chlorides are sharper than those of the bromides, the exciton peaks assigned to impurities (the lower multilayer compound) are rarely observed in the $m = 2$ and 3 chloride compounds.

The multilayer bromide compounds, $C_6Pb_mBr_{3m+1}$, films exhibited photoluminescence strong enough to detect with a naked eye even at room temperature. A strong and sharp peak of monolayer C_6PbBr_4 was observed at 406 nm with a full width of 120.1 meV at 295 K. This PL band is consistent with free exciton emission, because the Stokes shift of this film is as narrow as 40 meV. With respect to $C_6Pb_mBr_{3m+1}$ ($m = 2$ and 3) compounds, photoluminescence exhibited a pronounced spectral peak in the visible range with the maximum wavelengths at 437 and 459 nm, respectively. The emission of multilayer compounds was red-shifted by about 33 and 55 nm relative to that of the monolayer C_6PbBr_4. Although the absolute efficiency was not determined, the photoluminescence from the $m = 2$ and 3 spin-coated films was significantly weaker than that of the C_6PbBr_4 films. The exciton state in the multilayered perovskite compounds with thicker inorganic layers is less stable, and the emission associated with this state was correspondingly red-shifted because the bandgap energy and the exciton binding energy decrease with increasing m as a result of quantum confinement or dimensionality effects.

Conclusion

It has been demonstrated that the two-dimensional structure of lead halide perovskite compounds can be systematically varied over a wide range by the simple combination of organic alkylammonium and lead halide. The thin films of these perovskite compounds were fabricated by the conventional spin-coat method. Through this approach, it is possible to provide potential thin films for optical and electrical devices and to vary the key characteristics such as the distance between the inorganic

sheets, the thermal properties and stabilities, and the level of quantum confinement effect. There have been numerous reports related to these perovskite compounds. However, a comprehensive study of the simple two-dimensional layered perovskite compounds, $(C_nH_{2n+1}NH_3)_2(CH_3NH_3)_{m-1}Pb_mX_{3m+1}$ ($n = 2$, 3, 4, 6, and 10; X = Cl, Br, and I; $m = 1$, 2, 3, and ∞), involving the structural study, thermal properties and stability, fundamental optical properties, and quantum confinement effect, has not yet been published. Although little success in the use of these materials in devices has been achieved thus far, much effort should be devoted to try to understand the structural, optical, and electrical properties in order to materialize the potential applications. This fundamental and other systematic studies have revealed many new scientific facts. The size of the halogen atom in the layered perovskite compounds affects not only the optical properties but also the formation of molecular cavity consisting of the organic component, therefore resulting in the different organization of alkyl chains corresponding to the cavity size. It was thought that the quantum confinement effect was independent on the depth of organic barrier layer with a certain of alkyl length. However, wave function percolation was observed with the $(C_2H_5NH_3)_2PbBr_4$ films even though the film formed a layered structure. Fine $(C_2H_5NH_3)_2PbX_4$ (X = Cl and I) films could not to be fabricated regardless of the sizes. Furthermore, fine multilayer perovskite compound films could be prepared by varying the spin-coating conditions. The ability to manipulate the multilayer structure in these compounds will make it possible to fine-tune the optical properties such as absorption and photoluminescence.

This work was supported by the Precursory Research for Embryonic Science and Technology (PRESTO) and Core Research for Evolutional Science and Technology (CREST) of the Japan Science and Technology Agency (JST). The authors gratefully acknowledge Dr. F. S. Howell for his help with English corrections.

References

1 C. B. Murray, C. R. Kagan, M. G. Bawendi, *Science* **1995**, *270*, 1335.

2 Y. Sorek, R. Reisfeld, I. Finkelstein, S. Ruschin, *Appl. Phys. Lett.* **1995**, *66*, 1169.

3 For a recent review: D. B. Mitzi, *Prog. Inorg. Chem.* **1999**, *48*, 1.

4 G. C. Papavassiliou, *Prog. Solid State Chem.* **1997**, *25*, 125.

5 Y. I. Dolchenko, T. Inabe, Y. Maruyama, *Bull. Chem. Soc. Jpn.* **1986**, *59*, 563.

6 S. S. Nagapetyan, Y. I. Dolchenko, E. R. Arakelova, V. M. Koshkin, Y. T. Strchkov, V. E. Schklover, *Russ. J. Inorg. Chem.* **1988**, *33*, 1614.

7 T. Ishihara, J. Takahashi, T. Goto, *Solid State Commun.* **1989**, *69*, 933.

8 D. B. Mitzi, *Chem. Mater.* **1996**, *8*, 791.

9 C.-Q. Xu, T. Kondo, H. Sakakura, K. Kumata, Y. Takahashi, R. Ito, *Solid State Commun.* **1991**, *79*, 245.

10 M. Era, S. Morimoto, T. Tsutsui, S. Saito, *Appl. Phys. Lett.* **1994**, *65*, 676.

11 K. Shibuya, M. Koshimizu, Y. Takeoka, K. Asai, *Nucl. Instrum. Methods Phys. Res., Sect. B* **2002**, *194*, 207.

12 Y. Takeoka, K. Asai, M. Rikukawa, K. Sanui, *Chem. Commun.* **2001**, 2592.

13 T. Matsui, A. Yamaguchi, Y. Takeoka, M. Rikukawa, K. Sanui, *Chem. Commun.* **2002**, 1094.

14 Y. Takeoka, M. Fukasawa, T. Matsui, M. Rikukawa, K. Sanui, *Chem. Commun.* **2005**, 378.

15 D. Weber, *Z. Naturforsch. B: Chem. Sci.* **1978**, *33*, 1443.

16 A. Oglish, D. Weber, *J. Chem. Phys.* **1987**, *87*, 6373.

17 Y. Takeoka, K. Asai, M. Rikukawa, K. Sanui, *Chem. Lett.* **2005**, *34*, 602.

18 J. Calabrese, N. L. Jones, R. L. Harlow, N. Herron, D. L. Thorn, Y. Wang, *J. Am. Chem. Soc.* **1991**, *113*, 2328.

19 G. C. Papavassiliou, A. O. Patsis, D. J. Lagouvardos, I. B. Koustselas, *Synth. Met.* **1993**, *55–57*, 3889.

20 G. C. Papavassiliou, I. B. Koutselas, *Synth. Met.* **1995**, *71*, 1713.

21 D. B. Mitzi, C. A. Field, W. T. A. Harrison, A. M. Guloy, *Nature* **1994**, *369*, 467.

22 D. B. Mitzi, S. Wang, C. A. Field, C. A. Chess, A. M. Guloy, *Science* **1995**, *267*, 1473.

23 A. Poglitsh, D. Weber, *J. Chem. Phys.* **1987**, *87*, 6376.

24 T. Ishihara, in *Optical Properties of Low-Dimensional Materials*, ed. by T. Ogawa, Y. Kanematsu, World Scientific, Singapore, **1995**, p. 288.